minerals

MDPI

Review

Abyssal Serpentinites: Transporting Halogens from Earth's Surface to the Deep Mantle

Lilianne Pagé * and Keiko Hattori

Department of Earth and Environmental Sciences, University of Ottawa, Ottawa K1N 6N5, Canada; khattori@uottawa.ca

* Correspondence: lpage097@uottawa.ca

Received: 3 December 2018; Accepted: 17 January 2019; Published: 20 January 2019

Abstract: Serpentinized oceanic mantle lithosphere is considered an important carrier of water and fluid-mobile elements, including halogens, into subduction zones. Seafloor serpentinite compositions indicate Cl, Br and I are sourced from seawater and sedimentary pore fluids, while F may be derived from hydrothermal fluids. Overall, the heavy halogens are expelled from serpentinites during the lizardite–antigorite transition. Fluorine, on the other hand, appears to be retained or may be introduced from dehydrating sediments and/or igneous rocks during early subduction. Mass balance calculations indicate nearly all subducted F is kept in the subducting slab to ultrahigh-pressure conditions. Despite a loss of Cl, Br and I from serpentinites (and other lithologies) during early subduction, up to 15% of these elements are also retained in the deep slab. Based on a conservative estimate for serpentinite thickness of the metamorphosed slab (500 m), antigorite serpentinites comprise 37% of this residual Cl, 56% of Br and 50% of I, therefore making an important contribution to the transport of these elements to the deep mantle.

Keywords: serpentinite; halogens; subduction; deep mantle

1. Introduction

The high water content and enrichment of fluid-mobile elements (FME) in arc magmas attest to their recycling from Earth's surface to the mantle. The subduction of hydrated rocks, including sediments, altered oceanic crust (AOC) and abyssal serpentinites, at convergent plate boundaries provides a mechanism for this recycling. Abyssal serpentinites, primarily composed of the hydrous phyllosilicate mineral serpentine, are formed by the hydration of mantle peridotites on or near the seafloor. Recent geophysical and geochemical data have emphasized their importance for a variety of subduction-zone-related phenomena, including seismic activity and the exhumation of ultrahigh-pressure (UHP) rocks [1]. Furthermore, the high water content (up to 13 wt%) and wide stability (>100 km) [2] of serpentinites make them effective vehicles for the transport of FME, including halogens, into the mantle. This article reviews the incorporation of F, Cl, Br and I by the oceanic lithosphere during seafloor alteration and discusses the importance of abyssal serpentinites for halogen transfer from the Earth's surface to the deeper mantle.

2. Halogens as Tracers of Geological Processes

The halogens (F, Cl, Br, I) are highly reactive, volatile elements primarily concentrating in Earth's surface reservoirs, such as seawater (Cl, Br) and sediments (F, Br, I). They are also abundant in arc magmas compared to oceanic ridge magmas [3–5]. In addition, high F contents have been reported in magmas originating from the deeper mantle, such as ocean island basalts (OIBs) [6] and kimberlites [7].

The halogens are relatively abundant in crustal rocks compared to mantle peridotites [8] because they are preferentially partitioned into the silicate melt during partial melting due to their

incompatibility with mantle minerals. Chlorine, Br and I are also highly soluble in aqueous fluids, while the solubility of F is low [9]. Owing to its smaller size and higher electronegativity, F is far more compatible in hydrous and nominally anhydrous minerals than the other halogens [10–12]. As a consequence of their variable abundances and compatibilities, the halogens and their ratios (i.e., Br/Cl, I/Cl and F/Cl) are useful for tracing fluid sources and their migration in a variety of geological settings [13]. The halogens, particularly Cl, are also important ligands to form soluble metal complexes that contribute to metal transport and formation of metal deposits [14].

3. Abyssal Serpentinite Formation

The composition and structure of the oceanic lithosphere is primarily controlled by the spreading rate along the Earth's >67,000 km [15] of oceanic ridges. At fast-spreading ridges (>5 cm/year) [16], the rate of magma supply exceeds that of plate divergence, and large quantities of mafic magmas are generated. This produces the classic "Penrose" style of oceanic lithosphere [17] where layers of pillow basalts, sheeted dykes and layered gabbros are overlain by variable sediment cover and underlain by mantle peridotite [18] (Figure 1A). This transition from gabbro to peridotite at ~6–7 km depth represents the seismic Mohorovicic discontinuity (Moho) [18]. Hydrated mantle peridotites are observed along fractures and faults, which expose deep sections of oceanic lithosphere, such as Siqueiros Fracture Zone [19].

In contrast, the oceanic lithosphere produced in slow- (2–5 cm/year) and ultraslow- (<2 cm/year) [16] spreading ridges, such as the Mid-Atlantic Ridge (MAR) and South West Indian Ridge (SWIR), is much more heterogeneous [18]. It is characterized by sea floor exposure of variably serpentinized mantle peridotite overlain by a thin layer of pillow basalt and sheeted dykes, as described for the MAR [20], or a tectonically thinned out layer of volcanic rocks underlain by up to 3 km of extensively serpentinized peridotite, as described for the SWIR [21] (Figure 1B). The rifting of plates at the ridges exposes mantle peridotites to hydration by seawater or submarine hydrothermal fluids yielding abyssal serpentinites, which may comprise up to 25% of the oceanic lithosphere formed at slow-spreading ridges [22]. In these cases, the seismic Moho at shallower depths (1–4 km) may represent the serpentinization front [23].

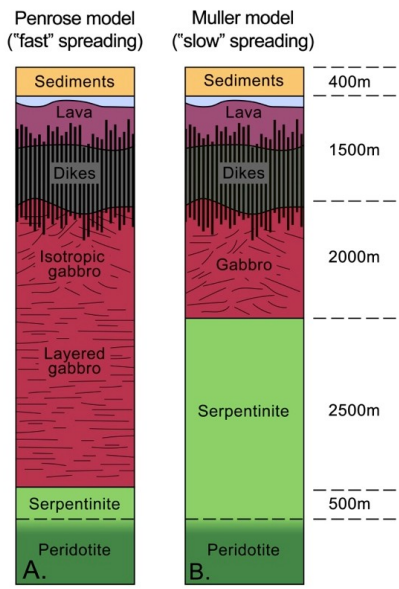

Figure 1. Simplified schematic diagram of representative cross sections of oceanic lithosphere produced at (**A**) fast- [17] and (**B**) slow- [21] spreading ridges. Serpentinite in the diagram represents either concentrated zones of serpentinization or diffuse serpentinization throughout the upper lithospheric mantle [24]. Oceanic lithosphere produced at slow- and ultraslow-spreading ridges is particularly heterogeneous, with serpentinites commonly outcropping on the ocean floor [20,22].

In addition to ridges, abyssal peridotites are hydrated at the outer rise near trenches by fluid infiltration along faults in the bending slab [25,26] (Figure 2). Estimates for the volume of abyssal serpentinites entering subduction zones range from a conservative 1–2% of the upper 10 km of lithospheric mantle [6] to 15% of the upper 30 km [26]. Serpentinization can also occur in mantle wedges by fluids released from subducting slabs [27] (Figure 2).

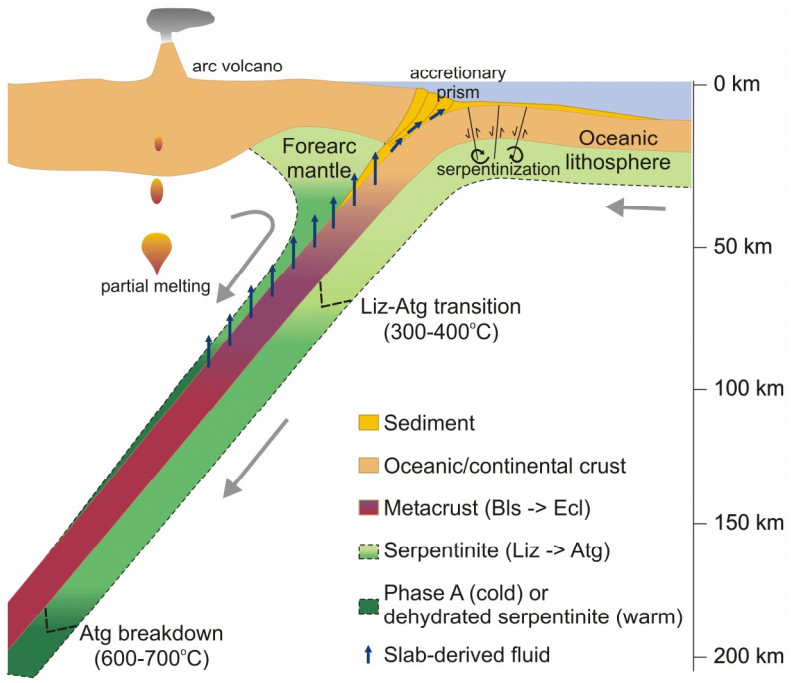

Figure 2. Schematic cross section of a cold subduction zone. Serpentinization of abyssal peridotite occurs on or near the seafloor and along fractures of the bending slab at the outer rise [25,26]. The approximate depths of the lizardite (Liz)–antigorite (Atg) transition [28] and antigorite decomposition [2] are based on a geothermal gradient of ~5 °C/km [29]. In cold subduction zones, fluids and fluid-mobile elements may persist in hydrous phase A after antigorite breakdown [30,31]. Bls: blueschist; Ecl: eclogite.

The formation of low-temperature (LT) serpentine phases, chrysotile and lizardite, occurs at temperatures below 400 °C [32]. The varieties of serpentine phases are due to the different ways for the mineral to adjust geometric strain between the tetrahedral and octahedral sheets [33]. Conditions that favour chrysotile formation over lizardite include a high water/rock ratio, isotopic shear stress and the hydration of microenvironments, such as veins and pores [32].

In close proximity of oceanic ridges, the fluid is dominated by seawater, as evidenced by serpentine $^{87}Sr/^{86}Sr$ ratios similar to that of present-day seawater [34]. Oxygen isotope compositions are also used to evaluate the nature of the hydrating fluid. For example, most serpentinites have $\delta^{18}O$ signatures between that of seawater (0‰$_{SMOW}$) and anhydrous peridotites (~+5–6‰$_{SMOW}$) [35]. However, some serpentinites formed at fast-spreading ridges, such as Hess Deep, have higher $\delta^{18}O$ values (~7‰), interpreted as evidence for hydration by evolved seawater, with possible contribution of magmatic fluids [36]. The existence of magmatic fluids at Hess Deep is also suggested by low $\delta^{13}C$ (−7.8‰ to −4.5‰) compared to 0‰ for dissolved carbonate in sea water and consistent with magmatic values [36]. During its transport from ridges to subduction zones, abyssal sediments deposit on the oceanic lithosphere. These abyssal sediments, and those derived from the overlying plate through erosion near trenches, can also influence the composition of serpentinization fluids along bend-related faults of the outer rise or within the subduction channel at shallow depths [37].

4. Incorporation of Halogens by Abyssal Serpentinites

Serpentinization of abyssal peridotites is characterized by moderate to strong enrichment of many FME, including halogens [38–48]. In situ analyses of serpentine grains from modern seafloor and obducted abyssal serpentinites show that concentrations of structurally bound Cl cover a large range (80 to 6000 ppm) [38,39,41,47], with an average of ~1500 ppm. This structurally bound Cl is considered to reside in the OH^- site of serpentine minerals [39]. Bulk rock analyses of abyssal serpentinites average slightly higher at ~2500 ppm Cl (Figure 3A) [40,42,44,46,49]. This extra Cl in the bulk rock data is likely in the form of Cl along grain boundaries [40].

The variable uptake of Cl by serpentinites has been attributed to several factors, including water/rock ratio, fluid salinity, primary minerals (i.e., olivine versus pyroxene) and temperature. Preliminary studies suggested different Cl contents of bulk serpentinites were the result of different water/rock ratios [42]; however, this is debated because of comparable Cl contents among serpentine grains from partially (20%) and fully serpentinized abyssal peridotites [47]. Furthermore, experimental serpentine products show similar Cl concentrations regardless of the water/rock ratio during the hydration of peridotites [50]. Fluid salinity also appears to have a negligible impact on the uptake of structurally bound Cl [50]; however, when Cl-poor serpentinites are equilibrated with saline fluids at ambient temperature and pressure, the uptake of structurally bound Cl in the serpentinites is proportional to the fluid salinity [51]. Chlorine contents have been shown to be higher in serpentine after orthopyroxene (bastite textures) compared to serpentine after olivine (mesh textures) in natural and experimental samples [39,49,51]. Compared to olivine, orthopyroxene contains significant Al replacing Si in the tetrahedral site [52]. Since Al has a larger ionic radius than Si, the substitution of Al for tetrahedral Si in lizardite reduces the distortion between the smaller tetrahedral and larger octahedral layers, which may allow the accommodation of the larger Cl ion (1.82 Å) in the OH^- site. The influence of temperature on Cl uptake is illustrated by an increase in the Cl content in serpentinite with increasing temperature up to a maximum of 200 °C and then a decrease in Cl contents at higher temperatures (300–500 °C) [50].

In contrast to Cl, there are fewer data available for Br and I in serpentinites due to their much lower concentrations. Electron microprobe analyses can determine the Cl content of most serpentine grains but not Br and I; therefore, data of these elements is mostly limited to bulk rock compositions. Recent bulk rock analyses suggest concentrations of 0.16–6.8 ppm Br (avg. 1.2 ppm; Figure 3A) and 0.016–2.6 ppm I (avg. 0.78 ppm; Figure 3B) in seafloor and obducted abyssal serpentinites [44,48,53]. Abyssal serpentinites have similar Br/Cl ratios to that of seawater, but their I/Cl ratios are much higher and overlap with those of sedimentary pore fluids (Figure 4A), suggesting a considerable contribution of sediments to serpentinizing fluids of abyssal serpentinites.

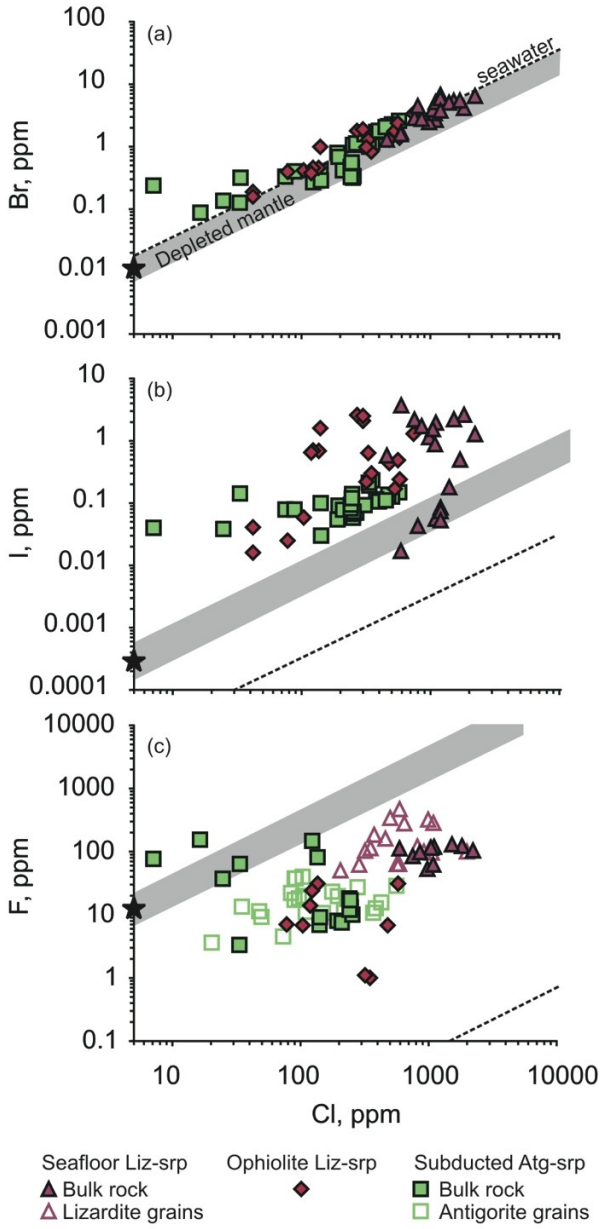

Figure 3. Halogen concentrations of seafloor and obducted abyssal lizardite serpentinites (Liz srp) and subducted antigorite serpentinites (Atg srp). Bulk serpentinite data are from [43,44,49,53]. In situ data of serpentine grains are from [34,43]. The F/Cl, Br/Cl and I/Cl ratios of the depleted mantle (grey fields) [6] and seawater (dashed lines) [54] are shown, along with the average concentrations of F, Cl, Br and I in the depleted mantle (black stars) [6]. Figures modified after [55]. (**a**) Bromine and Cl concentrations in all serpentinites are elevated with respect to the average depleted mantle but are strongly correlated along a linear trend defined by the Br/Cl ratio of the mantle and seawater, suggesting their coherent behaviour during serpentinization (hydration) and subduction (dehydration). On average, the obducted abyssal serpentinites having lower Br and Cl concentrations than the seafloor samples, and the subducted serpentinites have lower concentrations than the obducted samples. (**b**) All samples have elevated I concentrations with respect to the depleted mantle, and most samples also have I/Cl ratios greater than the mantle. Iodine and Cl broadly correlate among the seafloor and obducted abyssal serpentinites. The seafloor and obducted abyssal serpentinites have similar I concentrations, while their subducted counterparts extend to lower values. (**c**) Individual lizardite grains have higher F content than antigorite, but bulk rock values for lizardite- and antigorite serpentinites are similar. The higher F content of some subducted serpentinites may indicate an influx of F during antigorization from other dehydrating lithologies.

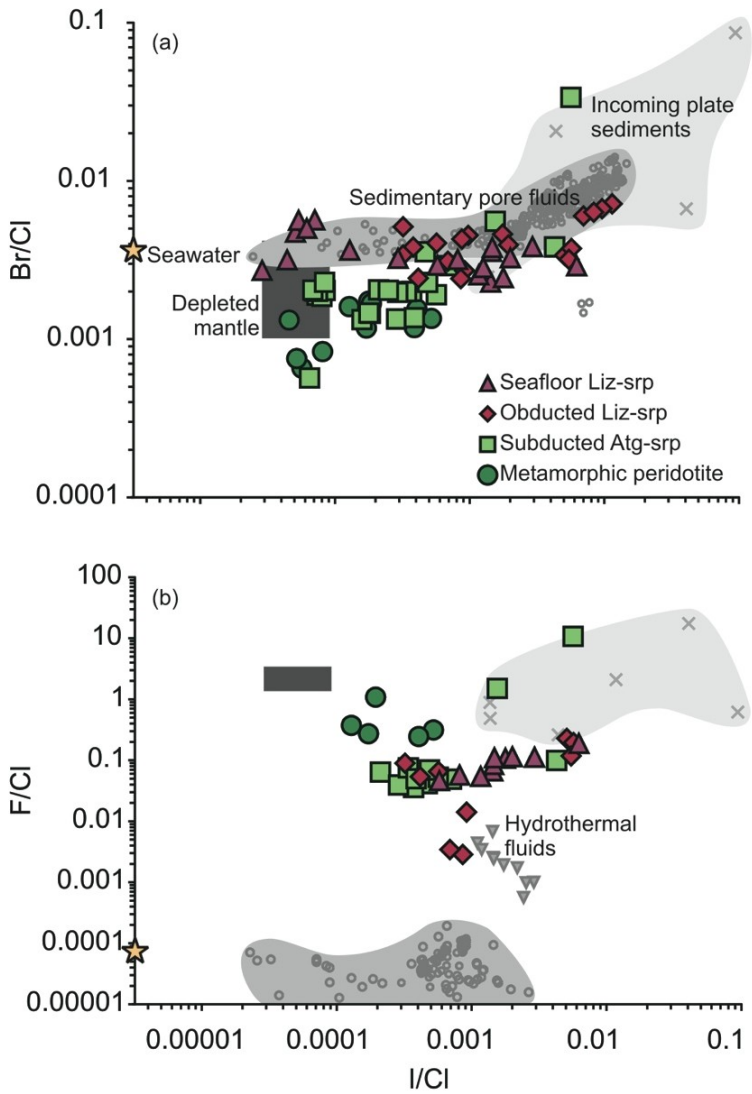

Figure 4. Halogen ratios of seafloor and obducted abyssal lizardite serpentinites (Liz srp), subducted antigorite serpentinites (Atg srp) and metamorphic peridotites after serpentinite dehydration. Bulk serpentinite data are from [43,44,48,53]. (**a**) Br/Cl and I/Cl ratios of the seafloor and obducted abyssal serpentinites overlap with those of sedimentary pore fluids (see [24] for review), while the Br/Cl ratios of the subducted serpentinites and metamorphic peridotites extend to lower values, similar to the depleted mantle [6]. (**b**) F/Cl ratios of all serpentinites are much higher than seawater [54], suggesting input from F-rich hydrothermal fluids (e.g., Escanaba Trough high $^{3}He/^{4}He$ pore fluids) [56] on the seafloor, or F mobilized from incoming plate sediments [53] and igneous lithologies during shallow subduction. On average, the subducted antigorite serpentinites and metamorphic peridotites have higher F/Cl ratios relative to their lizardite-bearing counterparts.

Few reports document the bulk F content in modern seafloor and obducted abyssal serpentinites. Obducted abyssal serpentinites in Tertiary subduction complexes in Dominican Republic and the Alps have concentrations (7–31 ppm F) [48,53] similar to those of the depleted mantle (12 ± 2 ppm) [6], whereas seafloor serpentinites from the Logatchev Hydrothermal Field along the Mid-Atlantic Ridge are enriched in F (50–130 ppm; Figure 3C). A similar enrichment is also observed for individual serpentine minerals from Logatchev and the Mid-Atlantic Ridge Kane (MARK) fracture zone (50 to 470 ppm; Figure 3C) [38,47]. The variable enrichment of F in abyssal serpentinites likely reflects the composition of the serpentinizing fluid. Seawater is generally low in F (<2 ppm) [54]; therefore, abyssal peridotites primarily hydrated by seawater are also expected to be low in F relative to

the other halogens. On the contrary, abyssal serpentinites formed near volcanic centres, such as Logatchev and the MARK area, may have elevated F contents and F/Cl ratios due to a contribution of hydrothermal fluids from volcanic rocks, which have been shown to have higher F/Cl ratios than seawater (Figure 4B) [56].

Additional F enrichment may occur during serpentinization at the outer rise or within the shallow subduction channel by F mobilized from overlying sediments or igneous lithologies. In general, F content and F/Cl ratios of sediment pore fluids are low (similar to seawater) due to the low solubility of F in aqueous fluids [9]. However, enrichment of F in water is expected during the dissolution of marine carbonates in water below the carbonate compensation depth, which contain up to 1700 ppm F [57] and high F/Cl ratios (~4–8) [58].

Similar to the heavy halogens, F is considered to reside in the serpentine OH^- site, but it may also be incorporated into the O^{2-} site due to their similar ionic radii. Charge imbalance is compensated for by the coupled substitution of Al^{3+} and F^- (1.33 Å) with Si^{4+} and O^{2-} (1.21 Å), as suggested for F in pyroxenes [10].

Recently published halogen budget calculations for a representative section of the oceanic lithosphere are based on a Penrose-type oceanic lithosphere typically produced at fast-spreading ridges [24]. It comprises 400 m of mature or lithified marine sediment, 1500 m of pillow basalts and sheeted dykes, 4500 m of gabbros and 500 m of serpentinites. In this model, serpentinites contribute 31% of the total I in the lithosphere, 23% Br, 26% Cl and 2% F (Figure 5). However, the degree of serpentinization is still poorly constrained, and this is considered a conservative lower limit for the contribution of serpentinites to the overall halogen budget of the oceanic lithosphere. Oceanic lithosphere produced at slow-spreading ridges likely contains a much larger volume of abyssal serpentinites. If we apply the Muller model [21] for oceanic lithosphere produced at slow-spreading ridges, which comprises up to 3000 m of serpentinized mantle peridotites, the contribution of serpentinites increases to 73% for I, 69% for Br, 78% for Cl and 14% for F (Figure 5). Mass balance calculations for a convergence rate of 5 cm/year, bulk plate density of 2.8 g/cm^3 and global trench length of 44,000 km [3] yield a global F influx of 6.41 $\times$ 10^{12} g/year regardless of the model used (Table 1). On the contrary, the total global influx of Cl, Br and I entering subduction zones with the Muller model (3.55 $\times$ 10^{13} g/year) doubles in comparison to that with the Penrose model (1.79 $\times$ 10^{13} g/year; Table 1), illustrating the importance for constraining the volume of serpentinites entering subduction zones.

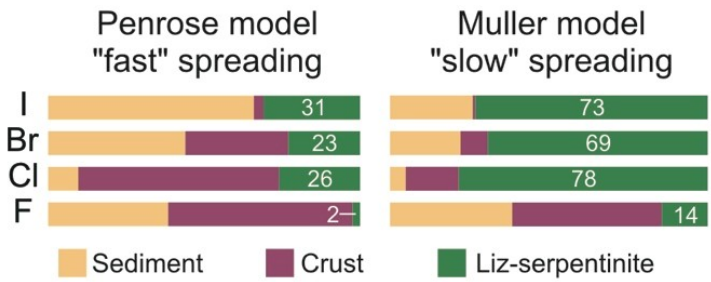

Figure 5. Summary of F, Cl, Br and I budget calculations for an incoming slab according to Penrose-type and Muller-type models of oceanic lithosphere produced at fast- and slow-spreading centers, respectively. The Penrose model consists of 400 m sediment, 6000 m igneous crust and 500 m lizardite serpentinites. The Muller model consists of 400 m sediment, 3500 m igneous crust and 300 m lizardite serpentinites. Average halogen concentrations for each unit are reported in Table 1. Numbers in bars denote the percent contribution of serpentinite to the total budget for each element.

Table 1. Summary of global mass balance calculations.

	Thickness, m *	Average Concentration, μg/g F	Cl	Br	I	Global Flux, g/year F ($\times 10^{12}$)	Cl ($\times 10^{12}$)	Br ($\times 10^{9}$)	I ($\times 10^{9}$)
Penrose model [1]									
Incoming slab [2]									
Sediment	400	1000	700	12	4.0	2.5	1.7	30	9.9
AOC, layer 2	1500	260	160	0.3	0.02	2.4	1.5	2.8	0.2
AOC, layer 3	4500	50	360	0.7	0.01	1.4	10	19	0.3
Liz serpentinite	500	50	1500	5.0	1.5	0.2	4.6	15	4.6
Bulk lithosphere	6900	151	419	1.6	0.4	6.4	18	67	15
	% in sediment					38	10	44	66
	% in AOC					59	64	33	3
	% in serpentinite					2	26	23	31
Metamorphosed slab									
Metasediment [3]	400	289	22	0.07	0.1	0.7	0.1	0.2	0.2
Eclogitic basalt [4]	1500	341	18	0.006	0.0005	3.2	0.2	0.1	0.004
Eclogitic gabbro [4]	4500	90	37	0.06	0.0007	2.5	1.0	1.8	0.02
Atg serpentinite [5]	500	42	235	0.8	0.09	0.1	0.7	2.6	0.3
Bulk lithosphere	6900	153	46	0.1	0.01	6.5	2.0	4.6	0.5
	% in sediment					11	3	4	45
	% in AOC					87	60	40	4
	% in serpentinite					2	37	56	50
	% retained in slab					101	11	7	4
Muller slow-spreading model [6]									
Incoming slab									
Sediment	400	1000	700	12	4.0	2.5	1.7	30	9.9
AOC, layer 2	1500	260	160	0.3	0.02	2.4	1.5	2.8	0.2
AOC, layer 3	2000	50	360	0.7	0.01	0.6	4.4	8.6	0.1
Liz serpentinite	3000	50	1500	5.0	1.5	0.9	28	92	28
Bulk lithosphere	6900	151	832	3.1	0.9	6.4	35	133	38
	% in sediment					38	5	22	26
	% in AOC					47	17	9	1
	% in serpentinite					14	78	69	73
Metamorphosed slab									
Metasediment	400	289	22	0.07	0.1	0.7	0.1	0.2	0.2
Eclogitic basalt	1500	341	18	0.006	0.0005	3.2	0.2	0.1	0.004
Eclogitic gabbro	2000	90	37	0.06	0.0007	1.1	0.5	0.8	0.01
Atg serpentinite	3000	42	235	0.8	0.09	0.8	4.3	16	1.6
Bulk lithosphere	6900	135	118	0.4	0.04	5.7	5.0	17	1.8
	% in sediment					12	1	1	13
	% in AOC					74	12	5	1
	% in serpentinite					13	87	94	86
	% retained in slab					90	14	12	5

[1] Thicknesses of lithological units from [24]; [2] Compilation of halogen concentrations of sediments, AOC and lizardite serpentinites of incoming slab from [24] and references therein; [3] Himalayan Tso Morari UHP sediments (unpublished data of Page, Hattori and Guillot, 2019); sampling and bulk chemistry described in [59]; halogen contents determined using methodology described in [48,60]; [4] Halogen data for eclogitic basalt and gabbro from Western Alps [61]; [5] Halogen data for antigorite serpentinites from Dominican Republic and Western Alps [48,53]; [6] Thicknesses of lithological units from [21]; AOC: altered oceanic crust; Liz: lizardite; Atg: antigorite.

5. Halogen Behaviour During Serpentinite Subduction

Available data of FME for subducted abyssal serpentinites are mostly from oceanic lithosphere produced at slow-spreading ridges, such as serpentinites of the Greater Antilles extinct arc in Dominican Republic [48], ophiolitic massifs of the Western Alpine–Northern Apennine chain in Italy [41,43,44,47,53] and the Cerro del Almirez massif in Spain [55]. Buoyant oceanic lithosphere formed at such slow-spreading ridges subducts at shallow angles and forms accretionary prisms, where the upper portion of the incoming oceanic lithosphere with sediments is scraped off and obducted [62]. The remaining serpentinites (and oceanic crust) are subducted to form subducted abyssal serpentinites. The FME data of abyssal serpentinites from fast-spreading ridges are virtually

nonexistent, with the exception of those from Hess Deep of the Pacific plate [36]. To date, there is no data for their subducted equivalents; however, serpentinization of oceanic lithosphere from fast-spreading ridges is suggested along deep fracture zones and during infiltration of fluids along extensional faults at the outer rise [26]. These serpentinites likely reside much deeper in the oceanic lithosphere, stay cooler for much longer than those near the top of the slab and as a consequence may transport FME even deeper in the mantle than summarized in this section.

5.1. Lizardite–Antigorite Transition

During shallow (<15 km) subduction, abundant water is expelled from sediments during their compaction and refluxed back to the Earth's surface (Figure 2) [63,64], but water structurally bound in hydrous minerals remains in subducting metasediments, altered oceanic crust and serpentinites. As the slab descends, the lizardite +/− chrysotile transition to antigorite occurs at ~300–400 °C [28] and is considered to be accompanied by the release of additional water [32] and certain FME [65]. This is supported by much higher concentrations of Cl, Br and I in seafloor and obducted abyssal lizardite serpentinites than subducted abyssal antigorite serpentinites [41,48,53,55]. This is also in agreement with lower Cl contents in other subducted lithologies (i.e., metasediments and metabasites) compared to their pre-subduction equivalents [60,66–68]. The transition is temperature-dependent. Therefore, it may occur at relatively shallow depths, 20–30 km, in warm subduction zones (~15 °C/km), or much deeper (60–80 km) in cold subduction zones (~5 °C/km; Figure 2).

Some antigorite serpentinites display lower Br/Cl and I/Cl ratios compared to their lizardite-bearing counterparts (Figure 4A), suggesting a preferential loss of Br and I relative to Cl during the serpentine phase transition [44,53,55], whereas others have slightly higher ratios (Figure 4A) [48]. Given the limited data available for HP serpentinites and the uncertainty regarding the exact composition of their protoliths, it is difficult to fully assess these subtle differences in halogen behaviour. The wide range of serpentinite compositions likely reflects variations in the timing and sources of serpentinization. Differences in halogen behaviour may also be attributed to different geothermal gradients and, consequently, varying depth of stability of host minerals among subduction zones. Regardless of these differences, overall, all studies indicate a loss of the heavy halogens during the transformation to antigorite. The halogens released from the slab during shallow subduction may be refluxed back to the ocean or transferred to the overlying mantle wedge where they are incorporated into forearc mantle serpentinites. Shallow (<25 km) forearc serpentinites have elevated halogen concentrations relative to the deleted mantle [44,48,69,70]. These serpentinites are considered an important transient reservoir for the halogens and other FME in the mantle wedge [71], and their dehydration in the deeper mantle may influence partial melting and volcanic front formation, as indicated by their similar FME enrichment patterns to those of arc magmas [27].

In contrast to the heavy halogens, bulk F contents of subducted abyssal antigorite serpentinites are similar to, if not higher than, those of obducted abyssal lizardite serpentinites (Figure 3C) [48,53]. Antigorite serpentinites also have consistently higher F/Cl ratios (Figure 4B), indicating a preferential retention of F and/or an additional influx during antigorite formation. During subduction, additional F may be mobilized from metasedimentary or crustal rocks. The improved accommodation of F relative to the heavier halogens is attributed to its smaller size and the crystallographic differences of lizardite and antigorite. In lizardite, the entire Si–O tetrahedral sheet is distorted to match the Mg–O octahedral sheet, resulting in a flat crystal structure, but in antigorite, individual Si–O tetrahedra are periodically reversed, yielding a more wavy structure with stronger bonds between layers and a tighter crystal structure overall [33]. As a result, the larger halogens may be more readily expelled from the hydroxyl sites during the phase transition [69], while the smaller F ion (1.33 Å), which has a similar ionic radius to OH^- (1.35 Å), is more likely to remain in the antigorite crystal structure. The retention of F in serpentine minerals during this transition is supported by in situ analyses of coexisting lizardite and antigorite grains from Western Alps that show similar F content in both serpentine phases [47].

5.2. Antigorite Dehydration

As the slab subducts farther into the mantle, antigorite eventually dehydrates to metamorphic peridotite at ~600–700 °C [2]. In warm subduction zones, this corresponds to a slab depth of ~80 km [30], but in cold subduction zones, the geothermal gradient is much smaller (~5 °C/km) [29], and abyssal serpentinites are thermodynamically stable to depths >150 km (Figure 2) [30,31]. Cold subduction zones are also characterized by much thicker oceanic lithosphere, resulting in a larger temperature difference (~200 °C) between the top and bottom of the slab [29]. Consequently, serpentinites of the lower section of the slab may remain stable to depths >200 km.

The dehydration of antigorite is accompanied by the release of fluids that become progressively depleted in Br and I relative to Cl [43,53], suggesting Br and I are preferentially lost during the early stages of antigorite breakdown. These fluids may be incorporated into the overlying mantle wedge, as evidenced by similar Br/Cl and I/Cl ratios to fluids in deep mantle wedge peridotites [72]. Yet, some Cl (<160 ppm), Br (<0.2 ppm) and I (<0.07 ppm) are retained in the dehydrated peridotite residues of subducting slabs and likely contained in desiccated fluid inclusions of olivine and pyroxene [55].

Fluorine residing in the antigorite OH^- site is also expected to be released during serpentinite dehydration, but F in the O^{2-} sites may be retained in nominally anhydrous minerals after antigorite decomposition. Indeed, high F (up to 130 ppm) has been reported in secondary olivine after antigorite decomposition [73]. The higher F in bulk HP serpentinites may also be attributed to the occurrence of Ti-clinohumite [53], a F-bearing accessory mineral of HP ultramafic rocks [74], or contained in chlorite as observed for the Cerro del Almirez (Spain) metamorphic peridotites [55].

6. Halogen Transfer to the Deeper Mantle

Preliminary mass balance calculations suggest nearly all subducted Cl is returned to surface reservoirs through arc volcanism [3,63]; however, these studies do not account for the significant Cl in abyssal serpentinites. More recent calculations that include abyssal serpentinites suggest inputs of Cl (and Br and I) in subduction zones may exceed volcanic outputs [53,75], and they also support the retention of nearly all subducted F (up to 95%) beyond subarc depths.

Here we show that subducted serpentinites are an important reservoir for halogens in the metamorphosed slab and a vehicle for their transport to the deeper mantle. Considering a model for oceanic lithosphere produced at fast-spreading ridges [24], serpentinites of 500 m thickness constitute 50% of residual I, 56% of Br, 37% of Cl and 2% of F in the eclogitized slab (Table 1; Figure 6). Yet, as previously mentioned, the volume of serpentinized peridotites entering subduction zones is not well defined. If serpentinite thickness is considered to be 3000 m, which is more representative of oceanic lithosphere produced at slow-spreading ridges [21], the serpentinite contribution increases to 86% for I, 94% for Br, 87% for Cl and 13% for F (Table 1; Figure 6).

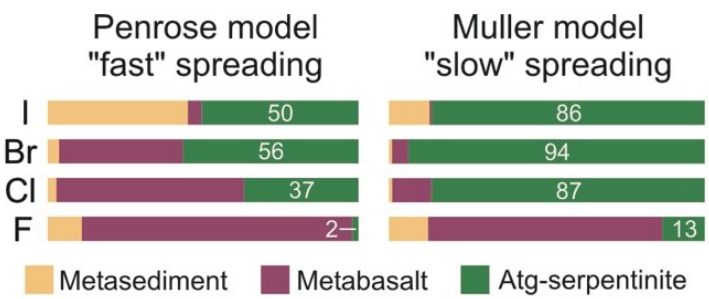

Figure 6. Summary of F, Cl, Br and I budget calculations for a metamorphosed slab according to Penrose-type and Muller-type models of oceanic lithosphere. See Figure 4 for descriptions of unit thicknesses. Average halogen concentrations for each unit are reported in Table 1. Numbers in bars denote the percent contribution of serpentinite to the total residual halogens in the slab.

Mass balance calculations confirm nearly all F is retained to HP-UHP conditions and suggest up to 14% Cl, 12% Br and 5% I may also be retained to such depths in the mantle, presumably beyond subarc depths (Table 1). These findings are in agreement with previous evidence for halogen retention beyond the depth of arc fronts based on their concentrations and ratios in magmas from the deeper mantle, including back-arc basin basalts (BABB) and ocean island basalts (OIB) [76–78]. Despite a loss of Cl, Br and I during early subduction, HP antigorite serpentinites can still retain appreciable amounts of these elements, along with significant F, compared to their peridotite protoliths [43,48,49,55,71]. Given its stability to ~200 km in cold subduction zones, antigorite may provide a reservoir for these elements to depths beyond those associated with most volcanic arcs (~100 km) [79], and some water and FME may be transported even deeper (up to 300 km) by hydrous phase A after antigorite decomposition (Figure 2) [31].

Author Contributions: Conceptualization, data curation, writing and figure preparation, L.P.; Advices and editing, K.H.

Funding: This research was funded by a Discovery Grant from the Natural Sciences and Engineering Research Council of Canada to Keiko Hattori.

Conflicts of Interest: The authors declare no conflict of interest.

References

1. Hirth, G.; Guillot, S. Rheology and tectonic significance of serpentinite. *Elements* **2013**, *9*, 107–113. [CrossRef]
2. Ulmer, P.; Trommsdorff, V. Serpentine stability to mantle depths and subduction-related magmatism. *Science* **1995**, *268*, 858–861. [CrossRef] [PubMed]
3. Straub, S.M.; Layne, G.D. The systematics of chlorine, fluorine, and water in Izu arc front volcanic rocks: Implications for volatile recycling in subduction zones. *Geochim. Cosmochim. Acta* **2003**, *67*, 4179–4203. [CrossRef]
4. Bouvier, A.S.; Metrich, N.; Deloule, E. Slab-derived fluids in the magma sources of St. Vincent (Lesser Antilles Arc): Volatile and light element imprints. *J. Petrol.* **2008**, *49*, 1427–1448. [CrossRef]
5. Sadofsky, S.J.; Portnyagin, M.; Hoernle, K.; van den Bogaard, P. Subduction cycling of volatiles and trace elements through the Central American volcanic arc: Evidence from melt inclusions. *Contrib. Mineral. Petrol.* **2008**, *155*, 433–456. [CrossRef]
6. Kendrick, M.A.; Hémond, C.; Kamenetsky, V.S.; Danyushevsky, L.; Devey, C.W.; Rodemann, T.; Jackson, M.G.; Perfit, M.R. Seawater cycled throughout Earth's mantle in partially serpentinized lithosphere. *Nat. Geosci.* **2017**, *10*, 222–228. [CrossRef]
7. Paul, D.K.; Buckley, F.; Nixon, P.H. Fluorine and chlorine geochemistry of kimberlites. *Chem. Geol.* **1976**, *17*, 125–133. [CrossRef]
8. Rudnick, R.L.; Gao, S. Composition of the continental crust. In *Treatise on Geochemistry*; Rudnick, R.L., Ed.; Elsevier: Oxford, UK, 2003; Volume 3, pp. 1–64. ISBN 0-08-043751-6.
9. Mahn, C.L.; Gieskes, J.M. Halide systematics in comparison with nutrient distributions in sites 1033B and 1034B, Saanich Inlet: ODP Leg 169S. *Mar. Geol.* **2001**, *174*, 323–339. [CrossRef]
10. Beyer, C.; Klemme, S.; Wiedenbeck, M.; Stracke, A.; Vollmer, C. Fluorine in nominally fluorine-free mantle minerals: Experimental partitioning of F between olivine, orthopyroxene and silicate melts with implications for magmatic processes. *Earth Planet. Sci. Lett.* **2012**, *337*, 1–9. [CrossRef]
11. Dalou, C.; Koga, K.T.; Shimizu, N.; Boulon, J.; Devidal, J.L. Experimental determination of F and Cl partitioning between lherzolite and basaltic melt. *Contrib. Mineral. Petrol.* **2012**, *163*, 591–609. [CrossRef]
12. Bernini, D.; Wiedenbeck, M.; Dolejš, D.; Keppler, H. Partitioning of halogens between mantle minerals and aqueous fluids: Implications for the fluid flow regime in subduction zones. *Contrib. Mineral. Petrol.* **2013**, *165*, 117–128. [CrossRef]
13. Pyle, D.M.; Mather, T.A. Halogens in igneous processes and their fluxes to the atmosphere and oceans from volcanic activity: A review. *Chem. Geol.* **2009**, *263*, 110–121. [CrossRef]
14. Seward, T.M.; Williams-Jones, A.E.; Migdisov, A.A. The Chemistry of Metal Transport and Deposition by Ore-Forming Hydrothermal Fluids. In *Treatise on Geochemistry*, 2nd ed.; Holland, H.D., Turekian, K.K., Eds.; Elsevier: Oxford, UK, 2014; Volume 13, pp. 29–57. ISBN 978-0-08-098300-4.

15. Bird, P. An updated digital model of plate boundaries. *Geochem. Geophys. Geosyst.* **2003**, *4*, 1–52. [CrossRef]
16. Dick, H.J.B.; Lin, J.; Schouten, H. An ultraslow-spreading class of ocean ridge. *Nature* **2003**, *426*, 405–412. [CrossRef] [PubMed]
17. Ophiolites. In *Proceedings of the Penrose Field Conference*; Geological Society of America: Minneapolis, MN, USA, 1972; Volume 12, pp. 24–25.
18. Dick, H.J.; Natland, J.H.; Ildefonse, B. Deep drilling in the oceanic crustand mantle. *Oceanography* **2006**, *19*, 72–80. [CrossRef]
19. Netland, J.H. Partial melting of a lithologically heterogeneous mantle: Inferences from crystallization histories of magnesian abyssal tholeiites from the Siqueiros Fracture Zone. *Geol. Soc. Spec. Publ.* **1989**, *42*, 41–70. [CrossRef]
20. Cannat, M.; Lagabrielle, Y.; Bougault, H.; Casey, J.; de Coutures, N.; Dmitriev, L.; Fouquet, Y. Ultramafic and gabbroic exposures at the Mid-Atlantic Ridge: Geological mapping in the 15 N region. *Tectonophysics* **1997**, *279*, 193–213. [CrossRef]
21. Muller, M.R.; Robinson, C.J.; Minshull, T.A.; White, R.S.; Bickle, M.J. Thin crust beneath ocean drilling program borehole 735B at the Southwest Indian Ridge? *Earth Planet. Sci. Lett.* **1997**, *148*, 93–107. [CrossRef]
22. Cannat, M.; Fontaine, F.; Escartín, J. Serpentinization and associated hydrogen and methane fluxes at slow spreading ridges. In *Diversity of Hydrothermal Systems on Slow Spreading Ocean Ridges*; Rona, P.A., Devey, C.W., Dyment, J., Murton, B.J., Eds.; American Geophysical Union: Washington, DC, USA, 2010; Volume 188, pp. 241–264.
23. Hess, H.H. History of ocean basins. In *Petrologic Studies*; Engel, A.E.J., James, H.L., Leonard, B.F., Eds.; Geological Society of America: Boulder, CO, USA, 1962; pp. 599–620.
24. Kendrick, M.A. Halogens in seawater, marine sediments and the altered oceanic lithosphere. In *The Role of Halogens in Terrestrial and Extraterrestrial Geochemical Processes*; Harlov, D.E., Aranovich, L., Eds.; Springer: Cham, Switzerland, 2018; pp. 591–648. ISBN 978-3-319-61665-0.
25. Kerrick, D. Serpentinite seduction. *Science* **2002**, *298*, 1344–1345. [CrossRef]
26. Ranero, C.R.; Morgan, J.P.; McIntosh, K.; Reichert, C. Bending-related faulting and mantle serpentinization at the Middle America trench. *Nature* **2003**, *425*, 367–373. [CrossRef]
27. Hattori, K.H.; Guillot, S. Volcanic fronts form as a consequence of serpentinite dehydration in the forearc mantle wedge. *Geology* **2003**, *31*, 525–528. [CrossRef]
28. Schwartz, S.; Guillot, S.; Reynard, B.; Lafay, R.; Debret, B.; Nicollet, C.; Lanari, P.; Auzende, A.L. Pressure–temperature estimates of the lizardite/antigorite transition in high pressure serpentinites. *Lithos* **2013**, *178*, 197–210. [CrossRef]
29. Tsujimori, T.; Sisson, V.B.; Liou, J.G.; Harlow, G.E.; Sorensen, S.S. Very-low-temperature record of the subduction process: A review of worldwide lawsonite Eclogites. *Lithos* **2006**, *92*, 609–624. [CrossRef]
30. Van Keken, P.E.; Hacker, B.R.; Syracuse, E.M.; Abers, G.A. Subduction factory: 4. Depth-dependent flux of H_2O from subducting slabs worldwide. *J. Geophys. Res. Solid Earth* **2011**, *116*, 1–15. [CrossRef]
31. Schmidt, M.W.; Poli, S. Experimentally based water budgets for dehydrating slabs and consequences for arc magma generation. *Earth Planet. Sci. Lett.* **1998**, *163*, 361–379. [CrossRef]
32. Evans, B.W. The serpentinite multisystem revisited: Chrysotile is metastable. *Int. Geol. Rev.* **2004**, *46*, 479–506. [CrossRef]
33. Evans, B.W.; Hattori, K.; Baronnet, A. Serpentinite: What, why, where? *Elements* **2013**, *9*, 99–106. [CrossRef]
34. Kimball, K.L.; Gerlach, D.C. Sr isotopic constraints on hydrothermal alteration of ultramafic rocks in two oceanic fracture zones from the South Atlantic Ocean. *Earth Planet. Sci. Lett.* **1986**, *78*, 177–188. [CrossRef]
35. Shanks III, W.C. Stable isotopes in seafloor hydrothermal systems: Vent fluids, hydrothermal deposits, hydrothermal alteration, and microbial processes. *Rev. Mineral. Geochem.* **2001**, *43*, 469–525. [CrossRef]
36. Früh-Green, G.; Plas, A.; Lécuyer, C. Petrologic and stable isotope constraints on hydrothermal alteration and serpentinization of the EPR shallow mantle at Hess Deep (Site 895). In Proceedings of the Oceanic Drilling Program, Scientific Results; Mével, C., Gillis, K.M., Allan, J.F., Meyer, P.S., Eds.; Ocean Drilling Program, Texas A&M University: College Station, TX, USA, 1996; Volume 147, pp. 255–291.
37. Deschamps, F.; Godard, M.; Guillot, S.; Hattori, K. Geochemistry of subduction zone serpentinites: A review. *Lithos* **2013**, *178*, 96–127. [CrossRef]
38. Orberger, B.; Metrich, N.; Mosbah, M.; Mével, C.; Fouquet, Y. Nuclear microprobe analysis of serpentine from the mid-Atlantic ridge. *Nucl. Instrum. Methods Phys. Res. Sect. B* **1999**, *158*, 575–581. [CrossRef]

39. Anselmi, B.; Mellini, M.; Viti, C. Chlorine in the Elba, Monti Livornesi and Murlo serpentines: Evidence for sea-water interaction. *Eur. J. Mineral.* **2000**, *12*, 137–146. [CrossRef]
40. Sharp, Z.D.; Barnes, J.D. Water-soluble chlorides in massive seafloor serpentinites: A source of chloride in subduction zones. *Earth Planet. Sci. Lett.* **2004**, *226*, 243–254. [CrossRef]
41. Scambelluri, M.; Müntener, O.; Ottolini, L.; Pettke, T.T.; Vannucci, R. The fate of B, Cl and Li in the subducted oceanic mantle and in the antigorite breakdown fluids. *Earth Planet. Sci. Lett.* **2004**, *222*, 217–234. [CrossRef]
42. Barnes, J.D.; Sharp, Z.D. A chlorine isotope study of DSDP/ODP serpentinized ultramafic rocks: Insights into the serpentinization process. *Chem. Geol.* **2006**, *228*, 246–265. [CrossRef]
43. Kendrick, M.A.; Scambelluri, M.; Honda, M.; Phillips, D. High abundances of noble gas and chlorine delivered to the mantle by serpentinite subduction. *Nat. Geosci.* **2011**, *4*, 807–812. [CrossRef]
44. Kendrick, M.A.; Honda, M.; Pettke, T.; Scambelluri, M.; Phillips, D.; Giuliani, A. Subduction zone fluxes of halogens and noble gases in seafloor and forearc serpentinites. *Earth Planet. Sci. Lett.* **2013**, *365*, 86–96. [CrossRef]
45. Kodolányi, J.; Pettke, T. Loss of trace elements from serpentinites during fluid-assisted transformation of chrysotile to antigorite—An example from Guatemala. *Chem. Geol.* **2011**, *284*, 351–362. [CrossRef]
46. Kodolányi, J.; Pettke, T.; Spandler, C.; Kamber, B.S.; Gméling, K. Geochemistry of ocean floor and forearc serpentinites: Constraints on the ultramafic input to subduction zones. *J. Petrol.* **2011**, *53*, 235–270. [CrossRef]
47. Debret, B.; Koga, K.T.; Nicollet, C.; Andreani, M.; Schwartz, S. F, Cl and S input via serpentinite in subduction zones: Implications for the nature of the fluid released at depth. *Terra Nova* **2014**, *26*, 96–101. [CrossRef]
48. Pagé, L.; Hattori, K. Tracing halogen and B cycling in subduction zones based on obducted, subducted and forearc serpentinites of the Dominican Republic. *Sci. Rep.* **2017**, *7*, 17776–17785. [CrossRef] [PubMed]
49. Bonifacie, M.; Busigny, V.; Mével, C.; Philippot, P.; Agrinier, P.; Jendrzejewski, N.; Scambelluri, M.; Javoy, M. Chlorine isotopic composition in seafloor serpentinites and high-pressure metaperidotites. Insights into oceanic serpentinization and subduction processes. *Geochim. Cosmochim. Acta* **2008**, *72*, 126–139. [CrossRef]
50. Huang, R.; Sun, W.; Zhan, W.; Ding, X.; Zhu, J.; Liu, J. Influence of temperature, pressure, and fluid salinity on the distribution of chlorine into serpentine minerals. *J. Asian Earth Sci.* **2017**, *145*, 101–110. [CrossRef]
51. Huang, R.; Ding, X.; Lin, C.T.; Zhan, W.; Ling, M. Effect of saline fluids on chlorine incorporation in serpentine. *Solid Earth Sci.* **2018**, *3*, 61–66. [CrossRef]
52. Eggins, S.M.; Rudnick, R.L.; McDonough, W.F. The composition of peridotites and their minerals: A laser-ablation ICP–MS study. *Earth Planet. Sci. Lett.* **1998**, *154*, 53–71. [CrossRef]
53. John, T.; Scambelluri, M.; Frische, M.; Barnes, J.D.; Bach, W. Dehydration of subducting serpentinite: Implications for halogen mobility in subduction zones and the deep halogen cycle. *Earth Planet. Sci. Lett.* **2011**, *308*, 65–76. [CrossRef]
54. Li, Y.H. A brief discussion on the mean oceanic residence time of elements. *Geochim. Cosmochim. Acta* **1982**, *46*, 2671–2675. [CrossRef]
55. Kendrick, M.A.; Scambelluri, M.; Hermann, J.; Padron-Navarta, J.A. Halogens and noble gases in serpentinites and secondary peridotites: Implications for seawater subduction and the origin of mantle neon. *Geochim. Cosmochim. Acta* **2018**, *235*, 285–304. [CrossRef]
56. Gieskes, J.M.; Simoneit, B.R.; Goodfellow, W.D.; Baker, P.A.; Mahn, C. Hydrothermal geochemistry of sediments and pore waters in Escanaba Trough—ODP Leg 169. *Appl. Geochem.* **2002**, *17*, 1435–1456. [CrossRef]
57. Rude, P.D.; Aller, R.C. Fluorine mobility during early diagenesis of carbonate sediment: An indicator of mineral transformations. *Geochim. Cosmochim. Acta* **1991**, *55*, 2491–2509. [CrossRef]
58. Carpenter, R. Factors controlling the marine geochemistry of fluorine. *Geochim. Cosmochim. Acta* **1969**, *33*, 1153–1167. [CrossRef]
59. Guillot, S.; De Sigoyer, J.; Lardeaux, J.M.; Mascle, G. Eclogitic metasediments from the Tso Morari area (Ladakh, Himalaya): Evidence for continental subduction during India-Asia convergence. *Contrib. Mineral. Petrol.* **1997**, *128*, 197–212. [CrossRef]
60. Pagé, L.; Hattori, K.; de Hoog, J.C.; Okay, A.I. Halogen (F, Cl, Br, I) behaviour in subducting slabs: A study of lawsonite blueschists in western Turkey. *Earth Planet. Sci. Lett.* **2016**, *442*, 133–142. [CrossRef]
61. Hughes, L.; Burgess, R.; Chavrit, D.; Pawley, A.; Tartèse, R.; Droop, G.; Ballentine, C.J.; Lyon, I. Halogen behaviour in subduction zones: Eclogite facies rocks from the Western and Central Alps. *Geochim. Cosmochim. Acta* **2018**, *243*, 1–23. [CrossRef]

62. Guillot, S.; Hattori, K.; Agard, P.; Schwartz, S.; Vidal, O. Exhumation Processes in Oceanic and Continental Subduction Contexts: A Review. In *Subduction Zone Geodynamics. Frontiers in Earth Sciences*; Lallemand, S., Funiciello, F., Eds.; Springer: Berlin/Heidelberg, Germany, 2009; pp. 175–205. ISBN 978-3-540-87971-8.
63. Jarrard, R.D. Subduction fluxes of water, carbon dioxide, chlorine, and potassium. *Geochem. Geophys. Geosyst.* **2003**, *4*, 1–50. [CrossRef]
64. Rüpke, L.H.; Morgan, J.P.; Hort, M.; Connolly, J.A. Serpentine and the subduction zone water cycle. *Earth Planet. Sci. Lett.* **2004**, *223*, 17–34. [CrossRef]
65. Barnes, J.D.; Sharp, Z.D.; Fischer, T.P. Chlorine isotope variations across the Izu-Bonin-Mariana arc. *Geology* **2008**, *36*, 883–886. [CrossRef]
66. Marschall, H.R.; Altherr, R.; Gméling, K.; Kasztovszky, Z. Lithium, boron and chlorine as tracers for metasomatism in high-pressure metamorphic rocks: A case study from Syros (Greece). *Mineral. Petrol.* **2009**, *95*, 291–302. [CrossRef]
67. Selverstone, J.; Sharp, Z.D. Chlorine isotope behavior during prograde metamorphism of sedimentary rocks. *Earth Planet. Sci. Lett.* **2015**, *417*, 120–131. [CrossRef]
68. Debret, B.; Koga, K.T.; Cattani, F.; Nicollet, C.; Van den Bleeken, G.; Schwartz, S. Volatile (Li, B, F and Cl) mobility during amphibole breakdown in subduction zones. *Lithos* **2016**, *44*, 165–181. [CrossRef]
69. Wei, W.; Kastner, M.; Deyhle, A.; Spivack, A.J. Geochemical cycling of fluorine, chlorine, bromine, and boron and implications for fluid-rock reactions in Mariana forearc, South Chamorro Seamount, ODP Leg 195. *Proc. Ocean. Drill. Progr. Part B Sci. Results* **2005**, *195*, 1–23. [CrossRef]
70. Snyder, G.T.; Savov, I.P.; Muramatsu, Y. Iodine and boron in Mariana serpentinite mud volcanoes (ODP Legs 125 and 195): Implications for forearc processes and subduction recycling. *Proc. Ocean. Drill. Progr. Sci. Results* **2005**, *195*, 1–18. [CrossRef]
71. Pagé, L.; Hattori, K.; Guillot, S. Mantle wedge serpentinites: A transient reservoir of halogens, boron, and nitrogen for the deeper mantle. *Geology* **2018**, *46*, 883–886. [CrossRef]
72. Sumino, H.; Burgess, R.; Mizukami, T.; Wallis, S.R.; Holland, G.; Ballentine, C.J. Seawater-derived noble gases and halogens preserved in exhumed mantle wedge peridotite. *Earth Planet. Sci. Lett.* **2010**, *294*, 163–172. [CrossRef]
73. De Hoog, J.C.; Hattori, K.; Jung, H. Titanium-and water-rich metamorphic olivine in high-pressure serpentinites from the Voltri Massif (Ligurian Alps, Italy): Evidence for deep subduction of high-field strength and FME. *Contrib. Mineral. Petrol.* **2014**, *167*, 1–15. [CrossRef]
74. Lopez Sánchez-Vizcaíno, V.L.; Trommsdorff, V.; Gómez-Pugnaire, M.T.; Garrido, C.J.; Müntener, O.; Connolly, J.A. Petrology of titanian clinohumite and olivine at the high-pressure breakdown of antigorite serpentinite to chlorite harzburgite (Almirez Massif, S. Spain). *Contrib. Mineral. Petrol.* **2005**, *149*, 627–646. [CrossRef]
75. Barnes, J.D.; Manning, C.E.; Scambelluri, M.; Selverstone, J. The behavior of halogens during subduction-zone processes. In *The Role of Halogens in Terrestrial and Extraterrestrial Geochemical Processes*; Harlov, D.E., Aranovich, L., Eds.; Springer: Cham, Switzerland, 2018; pp. 545–590. ISBN 978-3-319-61665-0.
76. Workman, R.K.; Hauri, E.; Hart, S.R.; Wang, J.; Blusztajn, J. Volatile and trace elements in basaltic glasses from Samoa: Implications for water distribution in the mantle. *Earth Planet. Sci. Lett.* **2006**, *241*, 932–951. [CrossRef]
77. Kendrick, M.A.; Jackson, M.G.; Kent, A.J.; Hauri, E.H.; Wallace, P.J.; Woodhead, J. Contrasting behaviours of CO_2, S, H_2O and halogens (F, Cl, Br, and I) in enriched-mantle melts from Pitcairn and Society seamounts. *Chem. Geol.* **2014**, *370*, 69–81. [CrossRef]
78. Kendrick, M.A.; Arculus, R.J.; Danyushevsky, L.V.; Kamenetsky, V.S.; Woodhead, J.D.; Honda, M. Subduction-related halogens (Cl, Br and I) and H_2O in magmatic glasses from Southwest Pacific Backarc Basins. *Earth Planet. Sci. Lett.* **2014**, *400*, 165–176. [CrossRef]
79. Syracuse, E.M.; Abers, G.A. Global compilation of variations in slab depth beneath arc volcanoes and implications. *Geochem. Geophys. Geosyst.* **2006**, *7*, 1–18. [CrossRef]